IEEE Access
Multidisciplinary | Rapid Review | Open Access Journal

Received July 9, 2020, accepted July 28, 2020, date of publication August 27, 2020, date of current version September 18, 2020.

Digital Object Identifier 10.1109/ACCESS.2020.3019837

Robust Cognitive Radar Tracking Based on Adaptive Unscented Kalman Filter in Uncertain Environments

LEI ZHONG, (Member, IEEE), YONG LI, WEI CHENG, AND WEI ZHOU
School of Electronic Information, Northwestern Polytechnical University, Xi'an 710072, China

Corresponding author: Yong Li (ruikel@nwpu.edu.cn)

This work was supported by the Fundamental Research Funds for the Central Universities under Grant 3102019ZX015.

ABSTRACT This article presents an approach for cognitive radar to track the target state despite unknown statistics or sudden changes in noise exposed to uncertain environments. Given the prior knowledge or accurate estimation of the noise, cognitive radar can adaptively adjust the waveform in the transmitter by perceiving the environment. However, the measurement noise usually contains a priori unknown parameters which are difficult to be estimated, or the process noise without empirical model might be improperly configured. Besides, they may change abruptly or time-varying in practice. These issues are prone to occur in cognitive radar, leading to performance decline or failure in tracking ultimately. To alleviate this problem, a robust cognitive radar tracking method based on adaptive unscented Kalman filter (AUKF) is proposed in this article. Specifically, UKF is used to derive the cognitive mathematical model and estimate the states in nonlinear systems. Moreover, a robust adaptive mechanism is designed in the cognitive framework, which is independent of prior information. When the mismatch between the noise in the model and the noise in the environment emerges, the noise covariance can be corrected adaptively. To verify the efficiency of the scheme, maneuvering target tracking experiments are carried out in three uncertain noise scenarios. Simulation results show that the scheme outperforms the existing adaptive UKF and cognitive radar algorithms in terms of intelligence and robustness.

INDEX TERMS Cognitive radar, adaptive filtering, robust estimation, target tracking, uncertain noise.

I. INTRODUCTION

Since the concept of cognitive radar (CR) proposed in [1], concepts, frameworks, algorithms, and even experimental equipment have shown a process of gradual development. A knowledge-aided fully adaptive architecture was proposed in [2]. Thereafter, the first hardware device experiment was carried out, using the cognitive sensor/processor system framework [3], [4]. Many other existing works focused on waveform design and other technologies [5]–[7]. In terms of tracking methods, the Bayesian framework is considered to be the basic component of cognitive radar. In the beginning, the Kalman filter (KF) is used for target tracking in cognitive radar with a linear Gaussian environment [8]. In [3], [9], it is used in the framework design of cognitive radar, meanwhile, a cognitive radar engineering workspace is built to present the first experimental results, and the KF is used as the tracking filter again [4]. However, most of the tracking problems to be solved in radar are nonlinear or even non-Gaussian. For example, the multi-state transition of drone from hovering to maneuvering is often nonlinear, and the measurement noise is mostly flicker noise or heavy-tailed noise [10]. Cubature Kalman filter (CKF) is first used to deal with nonlinear problems in cognitive radar in [8]. Few works are taken the particle filter (PF) into account. A parallel structure of extended Kalman filter (EKF) and PF has been adopted to deal with the nonlinear state estimation, but it is still a standard KF in essence if the EKF is used in waveform selection [11]. It is only applicable for the estimation of weak nonlinear state because the state distribution is approximated by a Gaussian random variable (GRV), which is then propagated analytically through the first-order linearization of the nonlinear system. This will introduce large errors in the true posterior mean and covariance of the transformed GRV,

The associate editor coordinating the review of this manuscript and approving it for publication was Chengpeng Hao.

which may lead to suboptimal performance and sometimes divergence of the filter [Chap. 32 in 12].

It can be seen that KF or its variants are still the first choice for cognitive radar under the Bayesian framework, but few works are concerning about the unscented Kalman filter (UKF), used as a tracking method in cognitive radar. In fact, UKF can be used in severe nonlinear state and Gaussian noise [13]. It has a higher order of accuracy in the noise statistics estimation than the EKF, while would not add much calculation consumption compared to PF [14]. UKF and other traditional nonlinear estimation methods can estimate the state of nonlinear systems, while the noise parameter is assumed as a priori known, or it is configured properly. Otherwise, the filter may fail and the tracking results become inaccurate [15].

On the other hand, if the uncertain environment results in improper configuration, the parameters cannot be adaptive to the change of the environment. When the noise mismatch emerging in the tracking problem, adaptive KF (AKF), adaptive UKF (AUKF) and some other adaptive covariance-matching algorithms were developed to estimate the statistical properties of the system noise and solve the problem in an uncertain noise scenario [16], such as the methods based on multiple model [17], [18], the methods based on innovation or residual, and the windowing methods [19]–[21]. Moreover, an adaptive UKF extended the windowing concept from the linear KF to the nonlinear UKF [22]. In another novel adaptive UKF algorithm, the process noise covariance is adapted by a scaling factor [23]. However, most of the traditional adaptive filters have a small effect on robustness. Subsequently, the robust UKF is used to estimate the state when both process noise and environment noise are unknown [24]. Furthermore, a robust adaptive UKF is proposed in [13], based on that, an online fault-detection mechanism is adopted to reduce the computational burden in [25]. But from the perspective of cognitive radar, these new adaptive filtering algorithms are still ''passive'', even though they have the robust ability to handle uncertainties. In general, the conventional adaptive filters just solved the tracking problem in the receiver and used the feedforward methods to complete the optimization of the algorithm. They did not utilize the feedback mechanism from the receiver to the transmitter, and the interaction with the environment was not considered.

Cognitive radar can make full use of environmental information. It is usually assumed that the feedback of the environment can be reflected by the waveform selection [26], but the model selection indicates that environmental information is also considered as a priori known. However, it is difficult to grasp the environmental information in the measurement. The key factor that depends on the environment, especially the signal-to-noise ratio (SNR) estimated by pre-scanning in actual operation is unknown [9]. Also, only the measurement noise is known for the assumption, but not the process noise. In practice, the noise contained in the radar echoes changes along with the environment, so it is usually uncertain, while few works focus on unknown or uncertain noise in or out of cognitive radar systems.

Therefore, how to track the target in an uncertain environment is a huge challenge for cognitive radar when the noise is unknown or dynamic. In this article, a novel robust cognitive tracking algorithm based on AUKF is proposed to overcome the degradation of tracking performance, caused by environmental uncertainty. It adds a robust mechanism to the radar scene analyzer and Bayesian tracker to dynamically correct the covariance matrix of the noise and expected error. Meanwhile, it has a cognitive structure to keep the cost function of estimation minimum. The cognitive structure intelligently guarantees that the robust mechanism works with the smallest tracking error and optimal waveform parameters. On the other side, the robust mechanism ensures the cognitive optimal filter run in an accurate internal and external environment.

The contributions of this article lie in:

1) The framework of a cognitive tracking algorithm based on UKF is designed aiming at the scenario of state estimation in a nonlinear system. Target tracking can be carried out intelligently by using dynamic updates of environmental information and feedback of receiver to transmitter.

2) A robust method is developed in cognitive structure to filter the uncertain noise faced by the traditional UKF. The possible uncertain situations include the unknown, abruptly changed and time-varying noise, etc.

3) Feedback in the cognitive closed-loop requires the receiver to collect and extract environmental information accurately, but the parameter estimation may have low accuracy because of the uncertain noise. The cognitive radar system supplemented by the design of the robust mechanism is to be applied to practical applications.

The rest of this article is organized as follows. The mathematical model of the cognitive radar tracking framework is introduced in Section II, which includes the dynamic model and UKF based cognitive tracking method. Section III is devoted to the structure of the robust cognitive tracking algorithm based on AUKF, which optimizes the fault-detection mechanism and cognitive architecture respectively. The design of processing architecture characteristics by adaptive and robust is completed. The mathematical model of the proposed algorithm is also deduced in this section. Section IV shows the simulation implementation, taking the tracking of maneuvering cooperative turning model as an example. The state estimation scenario of the nonlinear system is constructed for simulation experiments. The last section presents the conclusion. The notations used in the remainder of this article are listed in Table 1.

II. COGNITIVE RADAR TRACKING FRAMEWORK

The cognitive cycle begins with the transmitter's scanning of the environment, and the echoes reflected from the environment are received into two modules, that is the scene analyzer and tracker. The former provides environmental information, and continuously updates the receiver with environmental

TABLE 1. Summary of notation.

$\boldsymbol{f}, \boldsymbol{h}$	State and measurement equation
$\mathbf{x}$	State vector
$\mathbf{z}$	Measurement vector
$\mathbf{v}, \mathbf{w}$	Process and measurement noise vector
$\mathbf{Q}, \mathbf{R}$	Process and measurement noise covariance
$\boldsymbol{\theta}, \boldsymbol{\Theta}$	Waveform parameter and waveform library
λ, ϕ	Envelope duration and chirp rate
$\Delta\lambda, \Delta\phi$	Step-size of envelope duration and chirp rate
$\mathbf{J}$	Fisher information matrix
$\mathbf{U}$	Scaled version of the Fisher information matrix
η, η_r	SNR of the echoes
σ_b	Standard deviation of the bearing measurement
$\mathbf{E}_k$	Expectation operation
$\mathrm{Tr}(\cdot)$	Trace of a matrix
$\boldsymbol{\mu}$	Innovation vector
$\mathrm{cov}(\cdot)$	Covariance
$\chi^2_{p,v}$	Threshold of the fault -detection mechanism
ζ, δ	Weighting factor
a, b	Tuning parameter based on the environments
$\boldsymbol{W}$	Weights of the sigma points
r	Observed distance between the radar and target
$\boldsymbol{\chi}$	Sigma sample points
n_x	Dimension of the state
κ	Scaling parameter

information. The latter performs tracking and decisions making for a potential target, and adjusts the waveform parameters based on the tracking results and decisions. The sensor continues to detect the environment, and this cycle repeats over and over to adapt to environmental changes through continuous interaction with the environment. The progress is called the perception-action cycle (PAC).

A. SYSTEM MODEL

The PAC comes from the cognitive mechanism of human beings. Taking this as a key part, a block diagram of the cognitive radar system is proposed in [1]. In the context of target tracking in cognitive radar, we adaptively design parameters of waveform according to the uncertain environments and the continuous correcting estimation of the noise to pursue robust performance and more accurate tracking. The framework of cognitive radar system based on AUKF and a mathematical model of the cognitive tracking method in uncertain environments are demonstrated in Fig. 1.

The system consists of three main components:

Waveform selection. The module in the left dotted frame is to adjust the waveform parameters, more details can be found in the scene actuator in the rest of this section.

Signal processor. It is worth noting that in the right dotted box we fuse the Bayesian-based tracking structure with the robust mechanism to form a robust and intelligent system, countering the uncertainty of the system and environment adaptively, which is the difference from the existing cognitive tracking systems. More details of the Bayesian framework are presented in this section, more details of the robust module can be found in section III.

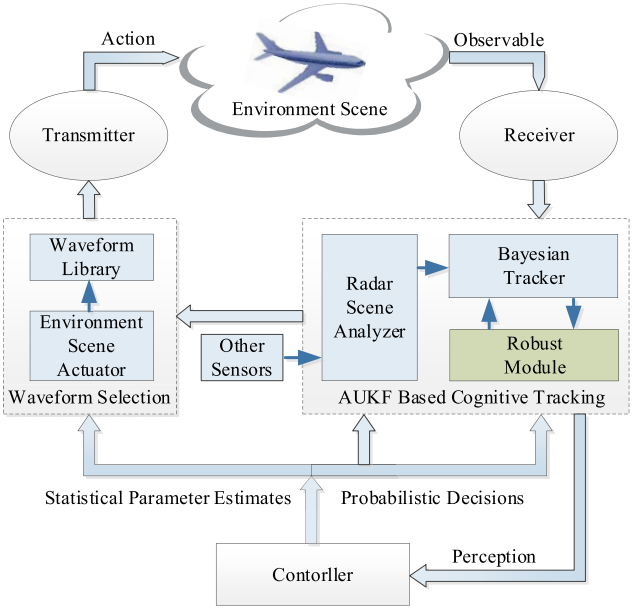

FIGURE 1. Block diagram of the cognitive radar system based on AUKF.

Controller. It determines the actions taken by the other two components, more details of the proposed cost function in it can be found in section III.

The objective of the framework is to focus attention on the nonlinear filtering in the uncertain environments, in which the unknown or dynamic process noise or measurement noise are taken into account. The dynamic model of a target with a nonlinear state can be given by

$$\mathbf{x}_{k+1} = \boldsymbol{f}_k(\mathbf{x}_k, \mathbf{v}_k) \tag{1}$$

where $\mathbf{x}_k$ is a n_x- dimensional state vector, k denotes the index of discrete-time, the expected covariance of process noise $\mathbf{E}\left\{\mathbf{v}_k \mathbf{v}_k^T\right\} = \mathbf{Q}_k$.

Radar scans the scene and achieves the observable vector $\mathbf{z}_k$. The measurement vector up to time t_k is denoted as $\mathbf{Z}_k \equiv \{\mathbf{z}_k, \mathbf{z}_k \cdots \mathbf{z}_k\}$. The model of sensor measurement is denoted by the nonlinear mapping of the $\mathbf{x}_k$

$$\mathbf{z}_k = \boldsymbol{h}(\mathbf{x}_k, \mathbf{w}_k) \tag{2}$$

where the expected covariance of measurement noise $\mathbf{E}\left\{\mathbf{w}_k \mathbf{w}_k^T\right\} = \mathbf{R}_k$.

$\mathbf{w}_k$ and $\mathbf{R}_k$ are related to the parameter $\boldsymbol{\theta}$ selected from the waveform library $\boldsymbol{\Theta}$ in the transmitter. We add the waveform parameter to the model of the sensor measurement, so Eq. (2) is replaced by $\mathbf{z}_k = \boldsymbol{h}(\mathbf{x}_k, \mathbf{w}_k(\boldsymbol{\theta}))$, the expected covariance $\mathbf{E}\left\{\mathbf{w}_k(\boldsymbol{\theta})\, \mathbf{w}_k(\boldsymbol{\theta})^T\right\} = \mathbf{R}_k(\boldsymbol{\theta})$.

In the actual scene of radar tracking, the measurement noise is usually complicated and varying with the change of the scene or time, and the parameters may be not constant. Obviously, the conventional tracking methodology with fixed parameters is susceptible to limitation, meanwhile, it is difficult to achieve the best tracking accuracy only by parameter adaptation inside the sensor without interacting with the environment.

B. COGNITIVE STRUCTURE

The cognitive structure includes the environment scene actuator, the radar scene analyzer, and the controller. They constitute the basic PAC. It needs to analyze the environment scene, select the waveform parameter, and control the next action taken by the receiver and transmitter. Since it involves interaction with the environment, we can consider it as an external adjustment.

1) COGNITIVE TRACKING METHOD BASED ON UKF

The radar scene analyzer in the cognitive radar system is composed of a sequential state estimator, as an input of the radar tracker, in which the Bayesian optimal filter is considered as the best choice for state tracking. The process is initialized in

$$f^{+}(\mathbf{x}_0) = q(\mathbf{x}_0) \tag{3}$$

The predicted density is computed from the Bayes-Markov recursion, denoted as

$$\begin{aligned} f^{-}(\mathbf{x}_k) &\equiv f(\mathbf{x}_k \,|\mathbf{Z}_{k-1}; \boldsymbol{\Theta}_k) \\ &= \int q(\mathbf{x}_k \,|\mathbf{x}_{k-1}; \boldsymbol{\theta}_k) f^{+}(\mathbf{x}_{k-1})\, d\mathbf{x}_{k-1} \end{aligned} \tag{4}$$

and the posterior density is computed using Bayes rule

$$\begin{aligned} f^{+}(\mathbf{x}_k) &\equiv f(\mathbf{x}_k \,|\mathbf{Z}_k; \boldsymbol{\Theta}_k) \\ &= \frac{f(\mathbf{z}_k \,|\boldsymbol{h}(\mathbf{x}_k); \boldsymbol{\theta}_k) f^{-}(\mathbf{x}_k)}{\int f(\mathbf{z}_k \,|\boldsymbol{h}(\mathbf{x}_k); \boldsymbol{\theta}_k) f^{-}(\mathbf{x}_k)\, d\mathbf{x}_k} \end{aligned} \tag{5}$$

Kalman filter is equivalent to the optimal filter under the linear and Gaussian assumptions. In our proposal, UKF is chosen as the approximation of the optimal filter under the nonlinear and Gaussian assumptions. The tracking algorithm based on UKF in cognitive radar is introduced for the following simulations, wherein, the standard UKF and its interface with basic cognitive tracking scheme are given in Appendix A.

2) COGNITIVE CONTROLLER AND SCENE ACTUATOR

We choose the duration of Gaussian pulse and the chirp rate to form the waveform parameter vector $\boldsymbol{\theta} = [\lambda, \phi]$. N_0 is selected to denote the spectral density of the complex noise envelope $\tilde{n}(t)$, SNR is known as $\eta = 2E_R/N_0$. The Fisher information matrix (FIM) can be found as

$$\mathbf{J}(\boldsymbol{\theta}_{k-1}) = \eta \mathbf{U}(\boldsymbol{\theta}_{k-1}) \tag{6}$$

where $\mathbf{U}(\boldsymbol{\theta}_{k-1})$ is a scaled version of the FIM. A symmetric matrix is defined as the form

$$\boldsymbol{\Gamma} \triangleq \operatorname{diag}\left[\frac{c}{2}, \frac{c}{4\pi f_c}\right] \tag{7}$$

where c is the speed of waveform propagation, f_c is the carrier frequency. The inverse of FIM is denoted by $\mathbf{J}^{-1}$, which is the unbiased estimator of the Cramér-Rao lower bound (CRLB) of the state estimation error covariance [27]. The measurement noise covariance can be denoted by [28]

$$\begin{aligned} \mathbf{R}(\boldsymbol{\theta}_{k-1}) &= \boldsymbol{\Gamma} \mathbf{J}^{-1}(\boldsymbol{\theta}_{k-1}) \boldsymbol{\Gamma} \\ &= \frac{1}{\eta} \boldsymbol{\Gamma} \mathbf{U}^{-1}(\boldsymbol{\theta}_{k-1}) \boldsymbol{\Gamma} \end{aligned} \tag{8}$$

When the linear frequency modulation (LFM) signal with Gaussian amplitude modulation is selected as the transmit waveform, [26] derived the covariance matrix further based on Eq. (8). In the modern radar tracking system, the standard deviation of bearing measurement is approximately expressed as [29]

$$\sigma_b = \frac{\Theta_{bw}}{k_m \sqrt{2\eta}} \tag{9}$$

where Θ_{bw} is the 3dB beamwidth of the radar antenna, k_m is the monopulse error slope. We introduce the augmented state vector, given as

$$\begin{aligned} &\mathbf{R}_k(\boldsymbol{\theta}_{k-1}) \\ &= \begin{bmatrix} \mathbf{R}(\boldsymbol{\theta}_{k-1}) & 0 \\ 0 & \sigma_b^2 \end{bmatrix} \\ &= \begin{bmatrix} \dfrac{c^2\lambda^2}{2\eta} & -\dfrac{c^2\phi\lambda^2}{2\pi f_c \eta} & 0 \\ -\dfrac{c^2\phi\lambda^2}{2\pi f_c \eta} & \dfrac{c^2}{(2\pi f_c)^2 \eta}\left(\dfrac{1}{2\lambda^2} + 2\phi^2\lambda^2\right) & 0 \\ 0 & 0 & \dfrac{\Theta_{bw}^2}{2\eta k_m^2} \end{bmatrix} \end{aligned} \tag{10}$$

The transmitting waveform scans the environment with the parameter $\boldsymbol{\theta}_{k-1}$. The receiver estimates the state with the previous value and current measurement and obtains the predicted value $\{\mathbf{x}_{k|k}, \mathbf{P}_{k|k}\}$. By a one-step prediction of $\{\mathbf{x}_{k|k}, \mathbf{P}_{k|k}\}$, $\{\hat{\mathbf{x}}_{k+1|k}, \mathbf{P}_{k+1|k}\}$ can be achieved and fed back to the transmitter. The error covariance matrix $\mathbf{P}_{k+1|k+1}$ of the predicted state with $\boldsymbol{\theta}_k$ can be calculated by $\mathbf{P}_{k|k}$.

The cost function is defined according to the mean-square error (MSE) of the expectation of tracking state

$$g(\mathbf{x}_k, \boldsymbol{\theta}_k) = \mathbf{E}_k\left[\left(\mathbf{x}_{k+1} - \hat{\mathbf{x}}_{k+1|k+1}\right)^T \left(\mathbf{x}_{k+1} - \hat{\mathbf{x}}_{k+1|k+1}\right)\right] \tag{11}$$

where $\hat{\mathbf{x}}_{k+1|k+1}$ is the posterior predictive value of the state estimation given waveform parameter. $\hat{\mathbf{x}}_{k+1|k+1}$ is related to $\mathbf{z}_{k+1}$ which is a nonlinear mapping of $\mathbf{x}_{k+1}$, so it is difficult to solve this expectation by integration, and the cost function is approximated as

$$g(\mathbf{x}_k, \boldsymbol{\theta}_k) \approx \operatorname{Tr}\left(\mathbf{P}_{k+1|k+1}\right) \tag{12}$$

The objective function is employed in the controller and sent to the scene actuator by the scene analyzer. The optimization problem of the controller can be denoted as

$$\theta_k^* = \arg\min_{\theta_k \in \mathbf{\Theta}} \left[\mathrm{Tr}\left(\mathbf{P}_{k+1|k+1} \right) \right] \tag{13}$$

The upper and lower limits of the waveform parameters are determined according to the transmitter specifications, and the waveform library can be obtained as

$$\mathbf{\Theta} = \{ \lambda \in [\lambda_{\min} : \Delta\lambda : \lambda_{\max}], \phi \in [\phi_{\min} : \Delta\phi : \phi_{\max}] \} \tag{14}$$

Finally, the scene actuator is to design or select the optimal waveform in the receiver for the next transmission.

III. ROBUST COGNITIVE RADAR TRACKING ALGORITHM BASED ON AUKF

The optimal waveform is selected according to Eq. (13), namely, the action taken by the transmitter is considered to be the best response to the environment perceived by the receiver.

The cognitive tracking algorithm based on UKF established above can solve most of the state estimation in high-dimensional nonlinear systems, and the feedback of the environment can be expressed by the character of the measurement noise. However, the SNR η in Eq. (6) which represents the environment characteristic in the algorithm is from prior information, or it may be mismatched with the actual situation. Besides, only $\mathbf{R}_k$ can be estimated by the waveform parameters but not $\mathbf{Q}_k$, and the $\mathbf{Q}_k$ may also be configured properly in an ideal practice but improperly in reality. In these cases, the general cognitive radar tracking method may fail to obtain accurate estimation results.

To address the challenge, the adjustment from the outside only by waveform adaptation is also not enough. It makes sense to couple the internal and external mechanisms for environment confrontation. Therefore, we propose a robust cognitive radar tracking algorithm based on AUKF and the structure of which is illustrated in Fig. 2. The algorithm adjusts the estimation of the noise parameter by a robust algorithm, which ensures that the cognitive estimator is performed based on accurate information of the sensor inside. Meanwhile, the algorithm guarantees the cost function of estimation keep minimum by a cognitive structure, which intelligently guarantees that the tracking error is smallest and the waveform parameters are optimal under corresponding noise parameters so that the robust mechanism can adjust the system parameters based on accurate external environmental information.

A. ADAPTIVE ADJUSTMENT OF NOISE STATISTIC

Inspired by the work in [13], a fault-detection mechanism is introduced to determine whether it is necessary to adjust the noise covariance matrices $\mathbf{Q}_k$ and $\mathbf{R}_k$. The fault-detection

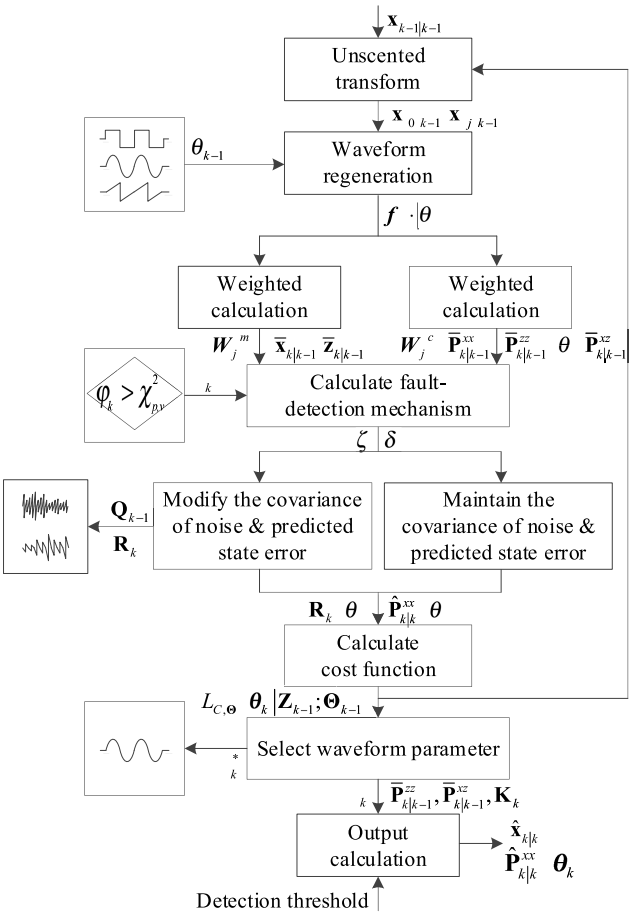

FIGURE 2. Schematic diagram of the proposed algorithm.

mechanism can be denoted by the statistical function

$$\varphi_k = \boldsymbol{\mu}_k^T \left[\bar{\mathbf{P}}_{k|k-1}^{zz} \right]^{-1} \boldsymbol{\mu}_k \tag{15}$$

where the innovation vector $\boldsymbol{\mu}_k = \mathbf{z}_k(\boldsymbol{\theta}_{k-1}) - \bar{\mathbf{z}}_{k|k-1}$ contains the newest information for the filter in the incoming measurement. The φ_k has a chi-square distribution with v degree of freedom where v is the dimension of $\boldsymbol{\mu}_k$. If the mechanism can detect the fault in the reliability of $1-p$, and the p is selected as

$$P\left(\varphi_k > \chi_{p,v}^2 \right) = p \tag{16}$$

then the corresponding threshold $\chi_{p,v}^2$ can be determined.

1) PROCESS NOISE ADJUSTMENT

The process noise can be derived from Eq. (1) using two approximations by linearization

$$\begin{aligned} \hat{\mathbf{w}}_{k-1} &= \hat{\mathbf{x}}_k - f\left(\hat{\mathbf{x}}_{k-1|k-1} \right) \approx \hat{\mathbf{x}}_k - \bar{\mathbf{x}}_{k|k-1} \\ &= \mathbf{K}_k \left(\mathbf{z}_k - \bar{\mathbf{z}}_{k|k-1} \right) \approx \mathbf{K}_k \boldsymbol{\mu}_k \end{aligned} \tag{17}$$

Then the process noise covariance is estimated with $\boldsymbol{\mu}_k$, similar work can be seen in [21], [23]

$$\begin{aligned} \mathbf{Q}_{k-1} &= \mathrm{cov}\left(\hat{\mathbf{w}}_{k-1} \right) \\ &= \mathbf{K}_k E\left[\boldsymbol{\mu}_k \boldsymbol{\mu}_k^T \right] \mathbf{K}_k^T \end{aligned} \tag{18}$$

Considering the calculation of $E\left[\boldsymbol{\mu}_k\boldsymbol{\mu}_k^T\right]$ need to average $\boldsymbol{\mu}_k\boldsymbol{\mu}_k^T$ over time and use the windowing method which will bring about the increasing computational burden, a one-step update method is adopted in this article to reduce the burden. The innovation covariance can be adjusted adaptively and updated as

$$\mathbf{Q}_{k-1} = (1-\zeta)\,\mathbf{Q}_{k-1} + \zeta\left(\mathbf{K}_k\boldsymbol{\mu}_k\boldsymbol{\mu}_k^T\mathbf{K}_k^T\right) \tag{19}$$

$$\zeta = \max\left\{\zeta_0, \left(\varphi_k - a\times\chi^2_{p,v}\right)/\varphi_k\right\} \tag{20}$$

where the weighting factor ζ is used to balance the last value and current estimation of $\mathbf{Q}_{k-1}$. $\zeta_0 \in (0,1)$, $a > 0$. We can put a known target in the unknown environment, and perform Monte Carlo in the training phase to obtain the value of a. So, a is a tuning parameter based on the environment. A small value of a means the update of $\mathbf{Q}_{k-1}$ is more sensitive to the new innovation, and vice versa, a large a means it is more likely to choose ζ_0, which is the lower limit of ζ. The new $\mathbf{Q}_{k-1}$ will be positive by using the update equation but without proof here.

2) MEASUREMENT NOISE ADJUSTMENT

Similar to the derivation of Eq. (18), the one-step update method instead of the windowing method is used to derive the measurement noise covariance, denoted as

$$\hat{\mathbf{R}}_k\left(\boldsymbol{\theta}_{k-1}\right) = \mathrm{cov}\left(\hat{\mathbf{v}}_k\right) = E\left(\boldsymbol{\varepsilon}_k\boldsymbol{\varepsilon}_k^T\right) + \hat{\mathbf{S}}^{zz}_{k|k} \tag{21}$$

where $\mathbf{v}_k = \mathbf{z}_k - h\left(\mathbf{x}_k\right)$ is from Equation (2), and a residual-based approach is used here to guarantee the matrix $\hat{\mathbf{R}}_k\left(\boldsymbol{\theta}_{k-1}\right)$ to be positive definite. The residual vector $\boldsymbol{\varepsilon}_k$ and the estimation item $\hat{\mathbf{S}}^{zz}_{k|k}$ can be denoted respectively as

$$\boldsymbol{\varepsilon}_k = \mathbf{z}_k - h\left(\hat{\mathbf{x}}_k^-\right) \tag{22}$$

$$\hat{\mathbf{S}}^{zz}_{k|k} = \sum_{j=0}^{2n_x} \boldsymbol{W}_j^{(c)}\left[\mathbf{z}_{(j)k|k} - \bar{\mathbf{z}}_{k|k}\right]\times\left[\mathbf{z}_{(j)k|k} - \bar{\mathbf{z}}_{k|k}\right]^T \tag{23}$$

The weighting factor δ is used here to balance the last value and current estimation of $\mathbf{R}_k\left(\boldsymbol{\theta}_{k-1}\right)$, which can be adjusted adaptively and updated as

$$\mathbf{R}_k\left(\boldsymbol{\theta}_{k-1}\right) = (1-\delta)\,\mathbf{R}_k\left(\boldsymbol{\theta}_{k-1}\right) + \delta\left[\boldsymbol{\varepsilon}_k\left(\boldsymbol{\varepsilon}_k\right)^T + \hat{\mathbf{S}}^{zz}_{k|k}\right] \tag{24}$$

$$\delta = \max\left\{\delta_0, \left(\varphi_k - b\times\chi^2_{p,v}\right)/\varphi_k\right\} \tag{25}$$

where $\delta_0 \in (0,1)$, b is a tuning parameter similar to a, $b > 0$. A small value of b means the $\mathbf{R}$ is more sensitive to the innovation, and vice versa, δ is closer to δ_0.

B. CORRECT ERROR COVARIANCE AND SNR ESTIMATION

More accurate error covariance can be derived after the $\mathbf{Q}_{k-1}$ and $\mathbf{R}_k$ have been updated, and the derivation is described by the following equations.

$$\bar{\mathbf{P}}^{xx}_{k|k-1} = \sum_{j=0}^{2n_x} \boldsymbol{W}_j^{(c)}\left[\chi_{(j)k|k-1} - \hat{\mathbf{x}}_k^-\right]\times\left[\chi_{(j)k|k-1} - \hat{\mathbf{x}}_k^-\right]^T + \mathbf{Q}_{k-1} \tag{26}$$

$$\bar{\mathbf{P}}^{xz}_{k|k-1} = \sum_{j=0}^{2n_x} \boldsymbol{W}_j^{(c)}\left[\chi_{(j)k|k-1} - \hat{\mathbf{x}}_k^-\right]\times\left[\mathbf{z}_{(j)k|k-1} - \bar{\mathbf{z}}_{k|k-1}\right]^T \tag{27}$$

$$\hat{\mathbf{P}}^{zz}_{k|k-1}\left(\boldsymbol{\theta}_{k-1}\right) = \hat{\mathbf{S}}^{zz}_{k|k} + \mathbf{R}_k\left(\boldsymbol{\theta}_{k-1}\right) \tag{28}$$

$$\hat{\mathbf{K}}_k = \bar{\mathbf{P}}^{xz}_{k|k-1}\left(\hat{\mathbf{P}}^{zz}_{k|k-1}\left(\boldsymbol{\theta}_{k-1}\right)\right)^{-1} \tag{29}$$

$$\bar{\mathbf{P}}^{xx}_{k|k}\left(\boldsymbol{\theta}_{k-1}\right) = \bar{\mathbf{P}}^{xx}_{k|k-1} + \hat{\mathbf{K}}_k\bar{\mathbf{P}}^{zz}_{k|k-1}\left(\boldsymbol{\theta}_{k-1}\right)\left(\hat{\mathbf{K}}_k\right)^T \tag{30}$$

By correcting the measurement noise covariance, the correct SNR η_k^* representing the current environmental information can be obtained by

$$\mathbf{R}_k\left(\boldsymbol{\theta}_{k-1}\right) = \frac{1}{\eta_k^*}\boldsymbol{\Gamma}\mathbf{U}^{-1}\left(\boldsymbol{\theta}_{k-1}\right)\boldsymbol{\Gamma} \tag{31}$$

C. UPDATE COST FUNCTION

The update equation for the tracking error covariance matrix at time $k+1$ is

$$\bar{\mathbf{P}}^{xx}_{k+1|k+1}\left(\boldsymbol{\theta}_k\right) = \bar{\mathbf{P}}^{xx}_{k+1|k} + \hat{\mathbf{K}}_{k+1}\bar{\mathbf{P}}^{zz}_{k+1|k}\left(\boldsymbol{\theta}_k\right)\left(\hat{\mathbf{K}}_{k+1}\right)^T \tag{32}$$

where $\bar{\mathbf{P}}^{zz}_{k+1|k}\left(\boldsymbol{\theta}_k\right)$ and $\hat{\mathbf{K}}_{k+1}$ are related to the measurement noise covariance matrix $\mathbf{R}_{k+1}\left(\boldsymbol{\theta}_k\right)$. We may replace them after the noise parameters are corrected by the robust mechanism

$$\bar{\mathbf{P}}^{zz}_{k+1|k}\left(\boldsymbol{\theta}_k\right) = \sum_{j=0}^{2n_x} \boldsymbol{W}_j^{(c)}\left[\mathbf{z}_{(j)k+1|k} - \bar{\mathbf{z}}_{k+1|k}\right]\times\left[\mathbf{z}_{(j)k+1|k} - \bar{\mathbf{z}}_{k+1|k}\right]^T + \mathbf{R}_{k+1}\left(\boldsymbol{\theta}_k\right) \tag{33}$$

$$\hat{\mathbf{K}}_{k+1} = \bar{\mathbf{P}}^{xz}_{k+1|k}\left(\bar{\mathbf{P}}^{zz}_{k+1|k}\left(\boldsymbol{\theta}_k\right)\right)^{-1} \tag{34}$$

We use Eq. (13) to define the optimal waveform parameter vector. Through the fine-tuning of external noise $\mathbf{R}$, the acquisition of internal process noise $\mathbf{Q}$, and the correction of the error covariance $\mathbf{P}_k^-$, we may replace Eq. (13) by

$$\theta_k^* = \arg\min_{\theta_k\in\mathcal{P}}\left[\mathrm{Tr}\left(\bar{\mathbf{P}}^{xx}_{k+1|k+1}\left(\boldsymbol{\theta}_k\right)\right)\right] \tag{35}$$

The next transmitted waveform is selected, and the current state estimation and its prediction covariance matrix is updated by

$$\hat{\mathbf{x}}_{k+1} = \bar{\mathbf{x}}_{k+1|k} + \mathbf{K}_{k+1}\left(\mathbf{z}_{k+1}\left(\boldsymbol{\theta}_k^*\right) - \bar{\mathbf{z}}_{k+1|k}\right) \tag{36}$$

$$\bar{\mathbf{P}}^{xx}_{k+1|k+1}\left(\boldsymbol{\theta}_k^*\right) = \bar{\mathbf{P}}^{xx}_{k+1|k} + \hat{\mathbf{K}}_{k+1}\bar{\mathbf{P}}^{zz}_{k+1|k}\left(\boldsymbol{\theta}_k^*\right)\left(\hat{\mathbf{K}}_{k+1}\right)^T \tag{37}$$

where $\mathbf{z}_{k+1}\left(\boldsymbol{\theta}_k^*\right)$ is the measurement corresponding to the parameter $\boldsymbol{\theta}_k^*$, given in Eq. (2) and (10).

Algorithm 1 Implementation of Robust Cognitive Radar Tracking Based on AUKF

Initialization

1 Select the waveform parameter $\boldsymbol{\theta}_0 = [\lambda_0, \phi_0]$

2 State $\hat{\mathbf{x}}_0 = \mu_0$, $\hat{\mathbf{P}}_0 = \Sigma_0$

Sigma point and weight value compute

3 Implement the steps in **Appendix B** to obtain $\mathbf{x}_{(j)k-1}$, $\boldsymbol{W}_j^{(m)}$, $\boldsymbol{W}_j^{(c)}$

4 for each $\boldsymbol{\theta}_{k-1} = [\lambda, \phi]$ compute one-step prediction of

5 $\mathbf{x}_{(j)k|k-1} = \boldsymbol{f}\left(\mathbf{x}_{(j)k-1}, \mathbf{v}_{k-1} | \boldsymbol{\theta}\right)$

6 $\bar{\mathbf{x}}_{k|k-1} = \sum_{j=0}^{2n_x} \boldsymbol{W}_j^{(m)} \mathbf{x}_{(j)k|k-1}$

7 $\bar{\mathbf{P}}_{k|k-1}^{xx} = \sum_{j=0}^{2n_x} \boldsymbol{W}_j^{(c)} \left[f\left(\mathbf{x}_{(j)k|k-1} | \boldsymbol{\theta}\right) - \bar{\mathbf{x}}_{k|k-1}\right] \times \left[f\left(\mathbf{x}_{(j)k|k-1} | \boldsymbol{\theta}\right) - \bar{\mathbf{x}}_{k|k-1}\right]^T + \mathbf{Q}_{k-1}$

Measurement update

8 $\mathbf{z}_{(j)k|k-1} = \boldsymbol{h}\left(\mathbf{x}_{(j)k|k-1}, \mathbf{w}_{k-1} | \boldsymbol{\theta}\right)$

9 $\bar{\mathbf{z}}_{k|k-1} = \sum_{j=0}^{2n_x} \boldsymbol{W}_j^{(m)} \mathbf{z}_{(j)k|k-1}$

10 $\bar{\mathbf{P}}_{k|k-1}^{zz}(\boldsymbol{\theta}) = \sum_{j=0}^{2n_x} \boldsymbol{W}_j^{(c)} \left[\mathbf{z}_{(j)k|k-1} - \bar{\mathbf{z}}_{k|k-1}\right] \times \left[\mathbf{z}_{(j)k|k-1} - \bar{\mathbf{z}}_{k|k-1}\right]^T + \mathbf{R}_k(\boldsymbol{\theta})$

11 $\bar{\mathbf{P}}_{k|k-1}^{xz} = \sum_{j=0}^{2n_x} \boldsymbol{W}_j^{(c)} \left[\mathbf{x}_{(j)k|k-1} - \bar{\mathbf{x}}_{k|k-1}\right] \times \left[\mathbf{z}_{(j)k|k-1} - \bar{\mathbf{z}}_{k|k-1}\right]^T$

Information update and state estimate

12 $\mathbf{K}_k \triangleq \bar{\mathbf{P}}_{k|k-1}^{xz} \left(\bar{\mathbf{P}}_{k|k-1}^{zz}(\boldsymbol{\theta})\right)^{-1}$

13 $\hat{\mathbf{P}}_{k|k}^{xx}(\boldsymbol{\theta}) = \bar{\mathbf{P}}_{k|k-1}^{xx} - \mathbf{K}_k \bar{\mathbf{P}}_{k|k-1}^{zz}(\boldsymbol{\theta}) (\mathbf{K}_k)^T$

14 Implement the robust algorithm as in **Appendix B** to obtain the corrected $\mathbf{Q}_{k-1}$, $\mathbf{R}_k(\boldsymbol{\theta})$, $\hat{\mathbf{x}}_{k|k}$ and $\hat{\mathbf{P}}_{k|k}^{xx}(\boldsymbol{\theta})$

15 Compute the cost function $\theta_k^* = \arg\min_{\theta} L_{C,\boldsymbol{\Theta}}(\theta_k | \mathbf{Z}_{k-1}; \boldsymbol{\Theta}_{k-1})$

16 Select the optimal waveform parameter $\boldsymbol{\theta}_k = \boldsymbol{\theta}_k^*$

Motion update

17 $\bar{\mathbf{x}}_{k|k-1} = \bar{\mathbf{x}}_{k|k-1}(\boldsymbol{\theta}_k)$

18 $\bar{\mathbf{P}}_{k|k-1}^{xx} = \bar{\mathbf{P}}_{k|k-1}^{xx}(\boldsymbol{\theta}_k)$

Measurement update

19 $\bar{\mathbf{P}}_{k|k-1}^{zz} = \sum_{j=0}^{2n_x} \boldsymbol{W}_j^{(c)} \left[\mathbf{z}_{(j)k|k-1} - \bar{\mathbf{z}}_{k|k-1}\right] \times \left[\mathbf{z}_{(j)k|k-1} - \bar{\mathbf{z}}_{k|k-1}\right]^T + \mathbf{R}_k(\boldsymbol{\theta}_k)$

20 $\bar{\mathbf{P}}_{k|k-1}^{xz} = \sum_{j=0}^{2n_x} \boldsymbol{W}_j^{(c)} \left[\mathbf{x}_{(j)k|k-1} - \bar{\mathbf{x}}_{k|k-1}\right] \times \left[\mathbf{z}_{(j)k|k-1} - \bar{\mathbf{z}}_{k|k-1}\right]^T$

Information update and state estimate

21 $\mathbf{K}_k \triangleq \bar{\mathbf{P}}_{k|k-1}^{xz} \left(\bar{\mathbf{P}}_{k|k-1}^{zz}(\boldsymbol{\theta}_k)\right)^{-1}$

22 $\hat{\mathbf{x}}_{k|k} = \bar{\boldsymbol{x}}_{k|k-1} + \mathbf{K}_k \left(\mathbf{z}_k - \bar{\mathbf{z}}_{k|k-1}\right)$

23 $\hat{\mathbf{P}}_{k|k}^{xx}(\boldsymbol{\theta}_k) = \bar{\mathbf{P}}_{k|k-1}^{xx} - \mathbf{K}_k \bar{\mathbf{P}}_{k|k-1}^{zz}(\boldsymbol{\theta}_k) (\mathbf{K}_k)^T$

24 Save the $\hat{\mathbf{x}}_{k|k}$ and $\hat{\mathbf{P}}_{k|k}^{xx}(\boldsymbol{\theta}_k)$

The parameter $\mathbf{R}$ is actively perceived by the cognitive structure to obtain the coarse adjustment and passively corrected by the internal robust mechanism to obtain the fine-tuning. The parameter $\mathbf{Q}$ is only corrected by the robust mechanism because it is just from the internal.

The robust module is added to the cognitive structure considering couple the internal and external mechanisms to form the proposed algorithm, which is summarized in Algorithm 1. If we use a fixed waveform, this can be reduced to the current robust AUKF, the interface of which with cognitive architecture is analyzed in detail in Appendix B.

IV. SIMULATION RESULTS

A. TARGET MODEL

A coordinated turn (CT) model with maneuvering properties is selected as the dynamic model of the target. As we know, the CT model is necessarily nonlinear if the turn rate is not a constant [30]. The system model is given by

$$\mathbf{x}_{k+1} = \mathbf{F}_k \mathbf{x}_k + \mathbf{v}_k \tag{38}$$

$\left[x_{1,k}, x_{2,k}, x_{3,k}, x_{4,k}\right]^T$ is selected to be the state vector $\mathbf{x}_k$ of the target, where $\left(x_{1,k}, x_{3,k}\right)$ and $\left(x_{2,k}, x_{4,k}\right)$ denotes the position and velocity respectively. $\mathbf{v}_k$ is the white Gaussian system noise, and the covariance matrix is given by $\mathbf{Q}$, the initial value of which is set as $\mathbf{Q}_0 = \text{diag}([\mathbf{Q}_{11}, \mathbf{Q}_{22}])$, $\mathbf{Q}_{11} = \mathbf{Q}_{22} = \sigma_{\mathbf{v}}^2 \begin{bmatrix} T^4/4 & T^3/2 \\ T^3/2 & T^2 \end{bmatrix}$, where $\sigma_{\mathbf{v}}^2$ is the variance of system noise. The state transition matrix is defined as

$$\mathbf{F}_k = \begin{bmatrix} \mathbf{F}_{11} & \mathbf{F}_{12} \\ \mathbf{F}_{21} & \mathbf{F}_{22} \end{bmatrix} \tag{39}$$

$$\mathbf{F}_{11} = \mathbf{F}_{22} = \begin{bmatrix} 1 & \dfrac{\sin \omega T}{\omega} \\ 0 \cos & \omega T \end{bmatrix} \tag{40}$$

$$\mathbf{F}_{12} = -\mathbf{F}_{21} = \begin{bmatrix} 1 & -\dfrac{1 - \cos \omega T}{\omega} \\ 0 & -\sin \omega T \end{bmatrix} \tag{41}$$

$\mathbf{z}_k = [r_k, \dot{r}_k, \theta_k]^T$ is selected as the observable vector, and the observation matrix denoted as

$$\boldsymbol{h}(\mathbf{x}_{k+1}) = \begin{bmatrix} \left(x_{1,k}^2 + x_{3,k}^2\right)^{1/2} \\ \left(x_{2,k}^2 + x_{4,k}^2\right)^{1/2} \\ \arctan\left(x_{3,k}/x_{1,k}\right) \end{bmatrix} + \mathbf{w}_k \tag{42}$$

Select Eq. (10) to be the model of $\mathbf{R}$. The fixed waveform parameter is set as $\lambda_0 = 50 \times 10^{-6}$s, $\phi_0 = 60 \times 10^9 Hz/s$, and the initial SNR is set as $\eta_0 = 16$, so $\mathbf{R}_0 = \mathbf{R}(\lambda_0, \phi_0, \eta_0)$. The initial position and velocity of the target are set as $\left(3.0 \times 10^3, 4.0 \times 10^3\right)$ m and $(100, 100)$ m/s respectively. The target takes 20s as a set of continuous turning times, and makes turning movements with the angular velocity of $\omega = 0.09^o/s, -0.04^o/s, -0.06^o/s, 0.08^o/s$ successively. $\mathbf{P}_0 = 10^4 \times diag([80, 2, 80, 2])$. The sampling period $T = 1$s. $\gamma_0 = \delta_0 = 0.2$. For the fault detection,

when the degree of freedom is 3 and the reliability level is 90% in chi-square distribution, the value of $\chi^2_{p,v}$ is taken as 6.25.

B. SIMULATION RESULTS

We explain and verify the proposed algorithm via the following examples of different scenarios. The measure for the assessed performance of different algorithms is the average root mean square error (ARMSE) which is generally used to estimate the tracking accuracy, given as

$$\text{ARMSE}=\sqrt{\frac{1}{N_m K}\sum_{i=1}^{N_m}\sum_{k=1}^{K}\left[\left(\hat{x}^i_{1,k}-x_{1,k}\right)^2+\left(\hat{x}^i_{3,k}-x_{3,k}\right)^2\right]} \tag{43}$$

where K denotes the number of time steps, N_m denotes the simulation index, $\left(\hat{x}^i_{1,k},\hat{x}^i_{3,k}\right)$ denotes the estimated position of the target at the $k-th$ step in the $i-th$ simulation, and $\left(x_{1,k},x_{3,k}\right)$ denotes the true path of the target.

The adjustment of parameters a and b in the introduced fault-detection mechanism will affect the robustness of the current AUKF and the proposed algorithm. Therefore, it is also necessary to discuss the selection of the parameter value and the influence.

We use three sets of noise covariance matrices to denote three different sorts of unknown environments, that is, $(\mathbf{Q}^\circ, \mathbf{R}(\eta_0))$, $(100\mathbf{Q}^\circ, \mathbf{R}(100\eta_0))$, $(0.01\mathbf{Q}^\circ, \mathbf{R}(0.2\eta_0))$. Then let a and b alter from 1 to 10 respectively to run multiple times simulation experiments. Finally, we search for a smaller error to determine the corresponding parameter value. Unlike existing researches, we obtain a three-dimensional ARMSE plot by varying the value of both a and b. In this way, suitable parameters can be found in a wider scope.

The case of Fig. 3a has the minimum uncertainty because the initial noise is closest to the actual value. The overall trend of the error is that it decreases first and then increases, along with the increase of values of a and b, indicating that too large or too small value is not suitable for parameters. Observe from Fig. 3b that the promotion of the tracking performance is not significant after $a, b > 2$. Fig. 3c shows when $a, b > 3$ the performance curve of the proposed algorithm floats in a low range, as for the fix waveform, a large value may result in a worse improvement. Based on the above three situations, it is reasonable to select $a = 6$, $b = 5$ for the rest of the simulations.

Notice that this is not the final result, but just to illustrate the rationality of parameter selection. Considering choosing the same parameter value for comparing different approaches, we do not give an optimal solution but only a relatively better one. Besides, this parameter selection is only an offline method, except for that, we have the cognitive structure to be the on-line mechanism, which can guarantee the tracking recursion update according to the environment.

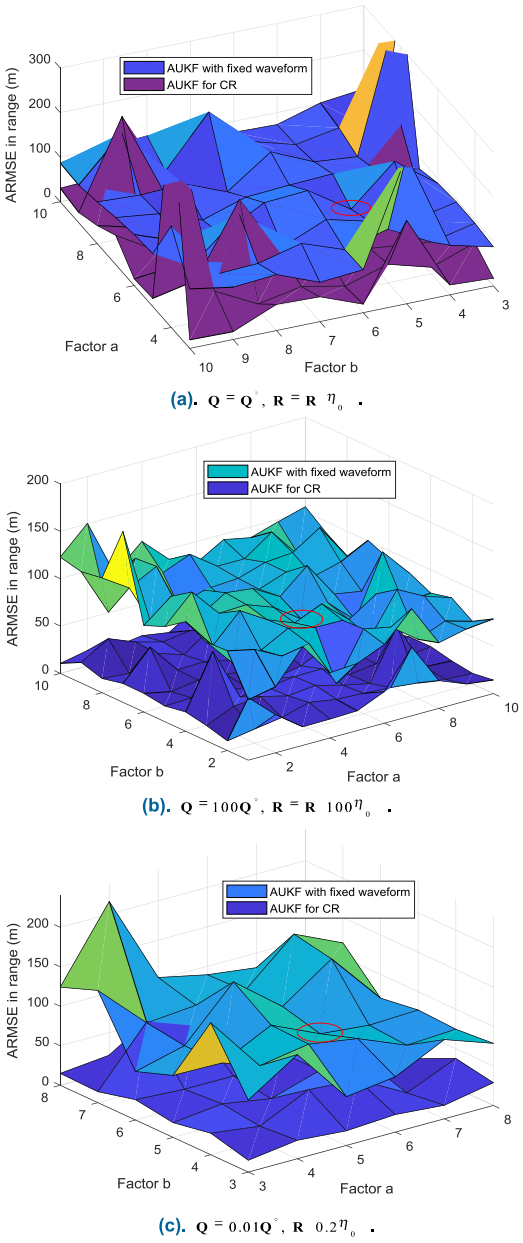

FIGURE 3. ARMSE in a range of different tuning parameters in different situations.

1) STATE ESTIMATION IN UNKNOWN NOISE

This article firstly considers the scenario that the noise is an unknown constant. It is necessary to design a variety of sets of process and measurement noise to represent uncertain features. $m = 0.5, 0.1, 1, 10, 50$, $n = 5, 2, 1, 0.5, 0.2$ are selected to construct the set $(\mathbf{Q}_0, \mathbf{R}_1 | \mathbf{Q}_0 = m \times \mathbf{Q}^\circ, \mathbf{R}_1 = \mathbf{R}(n \times \eta_0))$. The scenario is performed to compare the UKF with fixed waveform (FWF), AUKF with FWF, UKF for CR, and the proposed AUKF for CR. With 100 times Monte Carlo simulations, Table 2 – 5 gives the ARMSE of range estimation of different algorithms.

As expected, UKF with FWF has lower tracking accuracy than the other methods. At the right of Table 2, that is, when

TABLE 2. Errors of UKF with FWF.

ARMSE		$\mathbf{R}_1 = \mathbf{R}(n \times \eta_0)$				
		n = 5	n = 2	n = 1	n = 0.5	n = 0.2
$\mathbf{Q}_0 = m \times \mathbf{Q}^\circ$	m = 0.5	83.34	73.11	60.74	75.51	99.68
	m = 0.1	84.77	66.59	50.17	61.50	89.77
	m = 1	82.63	62.66	19.04	71.18	90.38
	m = 10	87.47	74.14	54.30	78.90	94.18
	m = 50	97.88	78.30	61.69	80.30	102.67

TABLE 3. Errors of AUKF with FWF.

ARMSE		$\mathbf{R}_1 = \mathbf{R}(n \times \eta_0)$				
		n = 5	n = 2	n = 1	n = 0.5	n = 0.2
$\mathbf{Q}_0 = m \times \mathbf{Q}^\circ$	m = 0.5	34.44	39.52	32.73	45.99	78.71
	m = 0.1	26.23	35.41	25.19	39.19	68.72
	m = 1	34.68	33.39	16.78	26.90	45.97
	m = 10	44.36	38.27	34.57	47.02	51.01
	m = 50	47.24	44.61	43.96	61.82	62.25

TABLE 4. Errors of UKF for CR.

ARMSE		$\mathbf{R}_1 = \mathbf{R}(n \times \eta_0)$				
		n = 5	n = 2	n = 1	n = 0.5	n = 0.2
$\mathbf{Q}_0 = m \times \mathbf{Q}^\circ$	m = 0.5	38.03	39.69	33.07	43.18	75.95
	m = 0.1	31.52	37.65	26.15	37.18	69.97
	m = 1	34.89	32.92	13.48	35.95	46.04
	m = 10	50.09	40.68	36.11	52.08	58.25
	m = 50	66.05	65.25	61.77	57.02	70.76

the value of $\mathbf{R}$ is much higher than the actual value, the performance degrades rapidly. That means the environment noise has a huge influence on tracking. The AUKF with FWF takes advantage of the robust mechanism and has better tracking accuracy than UKF, so the left of Table 3 is less affected by the value of $\mathbf{Q}$ but the performance also degrades with the influence of the environment. UKF for CR is less affected by the value of $\mathbf{R}$ since it has a detection mechanism for the environment. The varying of $\mathbf{Q}$ is the main cause result in the performance degradation, even if the estimated SNR is different from the actuality. The ARMSE given by AUKF for CR is the lowest one. Observe from the left of Table 5, it can be seen that when the process noise is significantly different from the actual value, the algorithm has more obvious performance improvement compared with UKF for CR because of the robust module working cooperatively with the cognitive structure. This also indicates that the proposed algorithm is a good supplement to the cognitive radar tracking method.

The RMSE of the estimated states at each time step can be expressed as [31]

$$\mathrm{RMSE}\,(k) = \sqrt{\frac{1}{N_m}\sum_{i=1}^{N_m}\left[\left(\hat{x}_{1,k}^{i} - x_{1,k}\right)^2 + \left(\hat{x}_{3,k}^{i} - x_{3,k}\right)^2\right]} \tag{44}$$

TABLE 5. Errors of AUKF for CR.

ARMSE		$\mathbf{R}_1 = \mathbf{R}(n \times \eta_0)$				
		n = 5	n = 2	n = 1	n = 0.5	n = 0.2
$\mathbf{Q}_0 = m \times \mathbf{Q}^\circ$	m = 0.5	33.10	28.95	24.39	33.83	37.98
	m = 0.1	22.74	32.15	22.90	29.82	34.48
	m = 1	22.29	21.90	12.05	25.70	32.84
	m = 10	38.41	37.04	30.58	44.17	48.08
	m = 50	43.67	42.38	41.71	47.18	62.71

The RMSEs in Fig. 4. can be more intuitive to show the developing trend of errors over time, and the similar conclusions as in the table 2 - V can be obtained. UKF with FWF has a relatively large error as a whole, and the advantage of cognitive structure in UKF for CR is offset by the robustness in AUKF. However, when the time is long enough, the difference that whether the actual noise can be approached asymptotically or not will emerge gradually. Obviously, AUKF for CR has a significant performance improvement compared with the other algorithms in this scenario.

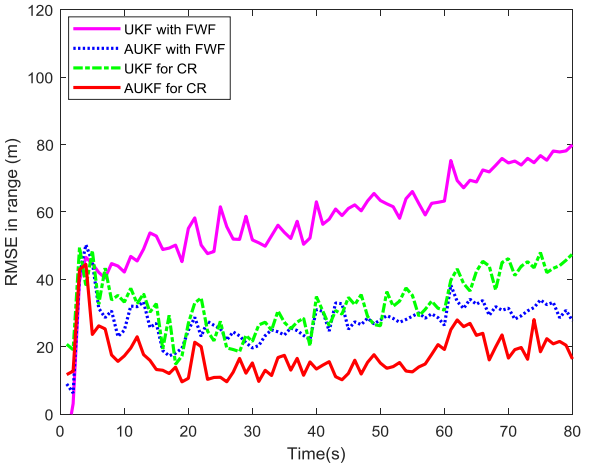

FIGURE 4. RMSE of estimated position, $\mathbf{Q} = 100\mathbf{Q}^\circ$, $\mathbf{R} = \mathbf{R}(100\eta_0)$.

2) STATE ESTIMATION IN DYNAMIC NOISE

In this case, the abrupt change of noise in an uncertain environment is considered. Other parameters required by the algorithms are the same as case 1). It is necessary to point out that in general simulation experiments, only one noise parameter would be discussed, i.e. $\mathbf{Q}$. However, we evaluate the robustness and intelligence degree of the algorithms under the circumstance that both $\mathbf{Q}$ and $\mathbf{R}$ vary, that is, ζ and δ will not be set as 0. We configure $\mathbf{Q}$ and $\mathbf{R}$ to represent different stages of uncertain environment, in the first case, $\mathbf{Q}$ is supposed to be a constant and $\mathbf{R}$ vary, denoted as

$$\begin{cases} \mathbf{Q}_0 = \mathbf{Q}^\circ, \mathbf{R}_1 = \mathbf{R}^\circ, & \mathrm{k} = 1, \cdots, 10 \\ \mathbf{Q}_0 = \mathbf{Q}^\circ, \mathbf{R}_1 = 0.2\mathbf{R}^\circ, & \mathrm{k} = 11, \cdots, 50 \\ \mathbf{Q}_0 = \mathbf{Q}^\circ, \mathbf{R}_1 = 5\mathbf{R}^\circ, & \mathrm{k} = 51, \cdots, 80 \end{cases} \tag{45}$$

Fig. 5 shows the RMSE curves corresponding to the four filters designed for the maneuvering case. When k = 1, ⋯, 20 with a priori known noise, all algorithms can track the target successfully. In the subsequent phase when **R** is reduced abruptly, the robust mechanism in AUKF with FWF shows its error correction performance, while the cognitive algorithm in UKF for CR has not yet shown an advantage of the adaption to the environment.

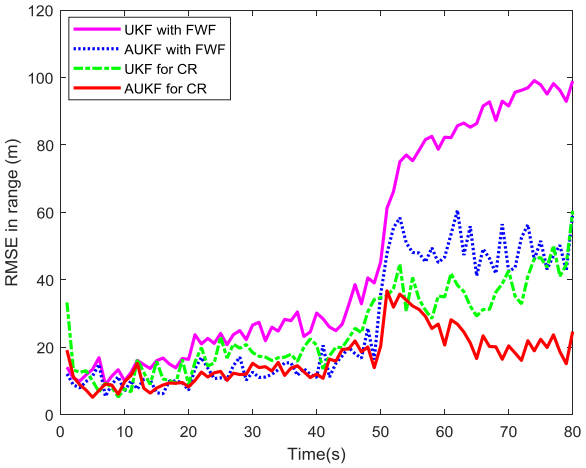

FIGURE 5. RMSE of estimated position, $\mathbf{Q}_0$ fixed.

In the stage when **R** increases suddenly, the AUKF with FWF can still converge the error, but the overall performance degrades rapidly. UKF for CR is not high because of the cognitive structure, which can reduce the effect of the measurement noise from the environment. The mastery of environmental information in time by both the UKF for CR and the AUKF for CR is the main reason why the proposed scheme outperforms the others. The real-time perception of the environment in the cognitive algorithm results in the performance degrades lightly, meanwhile, the robust mechanism makes the proposed scheme achieve fast convergence.

Another case of parameters is designed and denoted as follows

$$\begin{cases} \mathbf{Q}_0 = \mathbf{Q}^\circ, \mathbf{R}_1 = \mathbf{R}^\circ, & \mathrm{k} = 1, \cdots, 10 \\ \mathbf{Q}_0 = 0.5\mathbf{Q}^\circ, \mathbf{R}_1 = \mathbf{R}^\circ, & \mathrm{k} = 11, \cdots, 50 \\ \mathbf{Q}_0 = 10\mathbf{Q}^\circ, \mathbf{R}_1 = \mathbf{R}^\circ, & \mathrm{k} = 51, \cdots, 80 \end{cases} \tag{46}$$

It can be seen from Fig. 6 that all algorithms can accurately track the target when the noise is a priori known. When **Q** is reduced suddenly, the influence of the measurement noise plays a major role since the process noise is too small. Therefore, UKF for CR and AUKF for CR with cognitive structure can adapt to the environment noise and present better performance, whereas the adjustment of a robust mechanism for **Q** is not obvious. When the noise increases suddenly, the uncertainty of **Q** is to be the main factor affecting the tracking, while the cognitive structure has no superiority, and the disadvantage of UKF for CR lack of fault-detection mechanism is so evident. The error is high, especially when

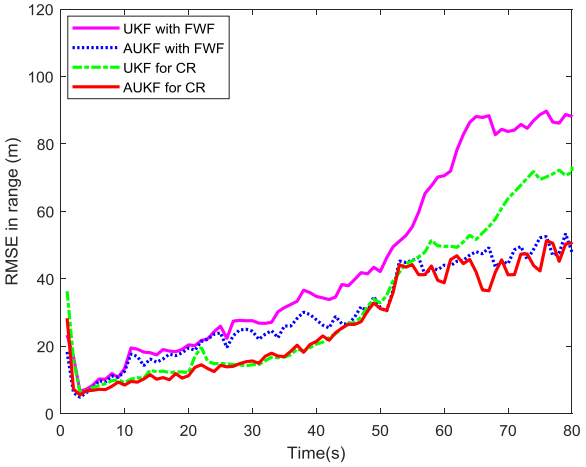

FIGURE 6. RMSE of estimated position, $\mathbf{R}_1$ fixed.

Q increases rapidly. Although the cognitive algorithm cannot take advantage of perceiving the environment, the robust mechanism makes the AUKF for CR no worse than AUKF with FWF, only the overall performance declines.

For more complicated scenarios, as shown in Table 6, **Q** and **R** change at the same time when $k = 10$ and $k = 50$. When the configured value is smaller than the actual one, the performance of UKF for CR is better than AUKF with FWF, but when the configured value is bigger than the actual one, the performance difference between them is reversed. Comparing the performance of AUKF for CR with other algorithms listed before, the results show the effectiveness and superiority of the proposed algorithm in nonlinear state estimation under uncertain system noise and environment noise.

TABLE 6. ARMSE at Different Time Step, m.

Time step	$\mathbf{Q}_0$	$\mathbf{R}_1$	UKF FWF	AUKF FWF	UKF for CR	AUKF for CR
k≤10	$\mathbf{Q}^\circ$	$\mathbf{R}^\circ$	10.23	9.75	9.63	9.36
10≤k≤50	$0.5\mathbf{Q}^\circ$	$0.2\mathbf{R}^\circ$	25.64	19.59	21.68	15.25
k>50	$10\mathbf{Q}^\circ$	$5\mathbf{R}^\circ$	70.51	52.32	48.19	40.02

3) STATE ESTIMATION IN TIME-VARYING NOISE

In the most complicated uncertain scenario, measurement noise changes in real-time with the transform of the environment, and Q value is fixed at this time. The energy of the received signal is inversely proportional to the fourth power of the target range [32], in light of the radar equation, the SNR model of the echoes can be defined by

$$\eta_r = (r_0/r)^4 \tag{47}$$

where r_0 represents the range between the radar and the target position where the SNR is 0dB, set as 100km in this article.

The tracking results are shown in Fig. 7, and the state estimation of the range rate is shown in Fig. 8, which shows the maneuvering of the target and the corresponding nonlinear dynamic characteristic of the state.

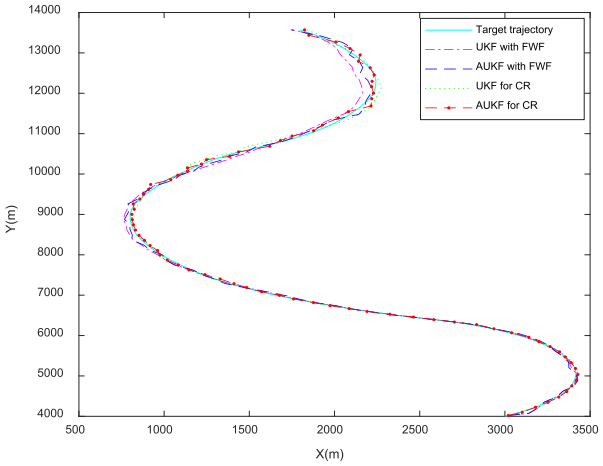

FIGURE 7. Comparison of tracking results of different algorithms.

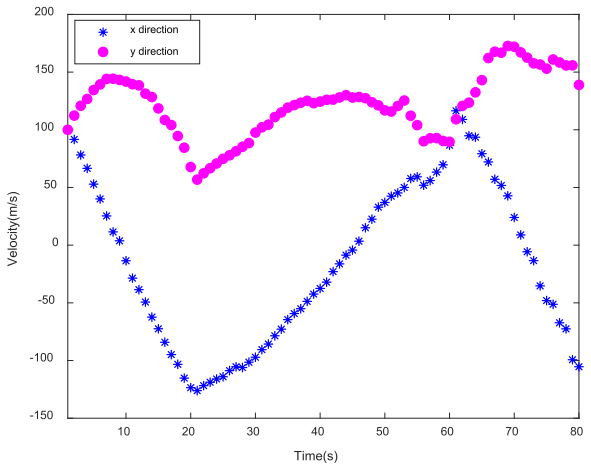

FIGURE 8. Variation of the velocity in the tracking scenario.

It can be seen from Eq. (47) that in the cognitive radar system the statistical characteristics of measurement changed with the adaptative of waveform parameters and the transformation of the environment. The SNR model is introduced, and the measurement noise will dynamically change with the target position. Fig. 9 shows the comparison of the accuracy in terms of RMSEs for range estimation. Similarly, conventional radar based on UKF cannot track the target accurately. In this scenario, the overall performance of cognitive radar based on UKF degrades since it has no fault-detection mechanism. For most of the time steps, it has a similar performance with the conventional radar based on AUKF. Especially when the noise uncertainty is weak, UKF for CR outperforms AUKF with FWF slightly, but when a strong uncertainty appears as shown in Fig. 8, the cognitive performance degrades. Our proposed scheme limits the overall

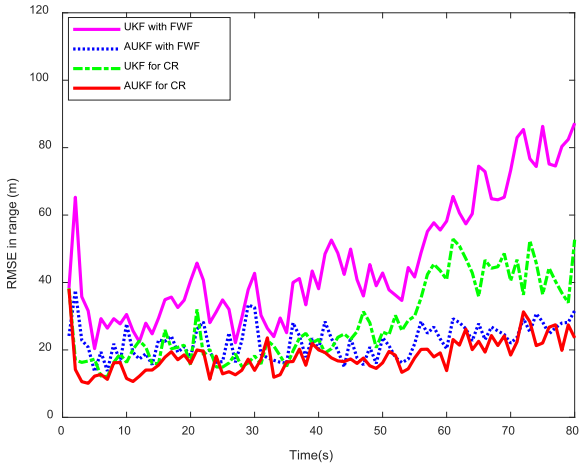

FIGURE 9. RMSE of estimated position.

magnitude of the error and always shows a superior real-time capability and robustness.

We compared the calculation time of various algorithms. Table 7 shows that UKF with FWF requires less calculation time than the others but has lowest tracking accuracy, UKF for CR has the similar accuracy with AUKF using FWF but spend more time, which shows a limitation of cognitive radar without the robustness, and AUKF for CR gives the lowest error while do not add much more calculation time, obviously as the most reasonable choice.

TABLE 7. Comparisons of performance metrics.

	UKF with FWF	AUKF with FWF	UKF for CR	AUKF for CR
Range ARMSE, m	49.03	20.85	28.92	16.12
Velocity ARMSE,m	9.35	4.96	6.13	3.24
Calculation time [a], s	0.0988	0.1124	1.0284	1.0458

[a]Simulations are executed on an Intel Core i5-3320M CPU 2.60 GHz personal computer with 10 GB of random-access memory PC.

This implies that the addition of robust modules does not generate too much extra calculation, and the main increase in calculation comes from the cognitive cycle. The AUKF adds the calculation time compared to UKF because the robust method needs to update the noise covariance recursively, but the one-step updating method saves a lot of calculation compared to general methods such us the windowing method, scale factor, etc., so, the addition of computational burden is slight. A similar situation can be seen in the comparison between UKF for CR and AUKF for CR. While the global dynamic optimization in the current cognitive architecture will inevitably lead to an increase in the calculation time. Therefore, we can get the conclusion that the robust module as a supplement to the cognitive system is competent.

The real-time variation of waveform parameters is shown in Fig. 10-11, including λ and ϕ.

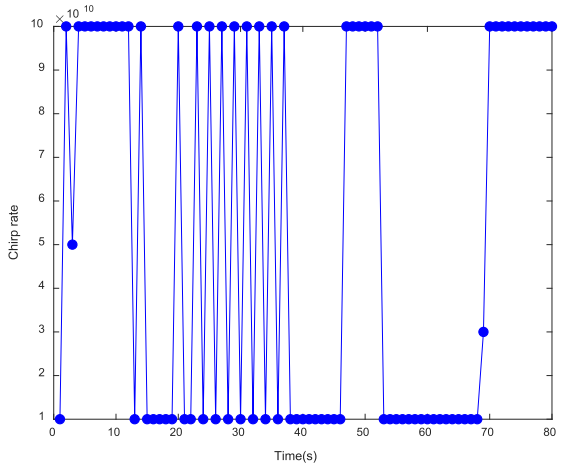

FIGURE 10. Waveform selection across time, on chirp rate.

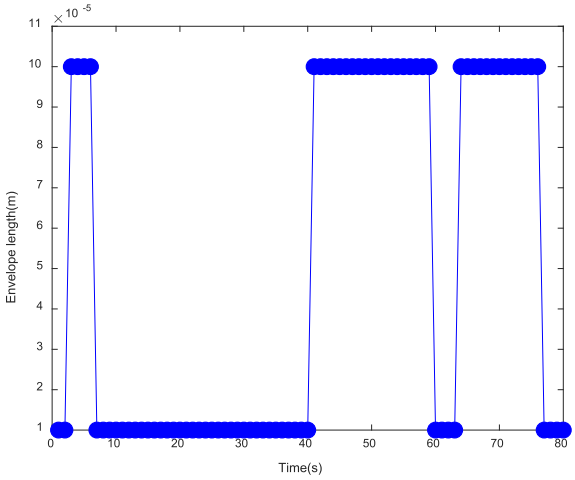

FIGURE 11. Waveform selection across time, on length of pulse envelope.

V. CONCLUSION

The problem of maneuvering target tracking with cognitive radar in uncertain environments is concentrated in this work. By the fact that the tracking accuracy of cognitive radar degrade when the environment noise is not estimated correctly, or the process noise is improperly configured. A novel cognitive tracking algorithm based on AUKF is proposed in this article. Specifically, a cognitive radar framework based on UKF has been presented which is allowed to deal with the general nonlinear problems. Furthermore, a robust algorithm was introduced to adaptively adjust the estimation of the process and measurement noise covariance. It could also help to perceive the environment in the cognitive structure with accurate parameter even in the uncertain scenarios. Simulation results illustrate that the presented cognitive radar tracking method based on AUKF outperformed the existing methods not only in estimation accuracy but also in robustness to resist the uncertain environment, including unknown, dynamic, and time-varying noise. The proposed method is expected to be used as a supplement to the existing tracking methods in cognitive radar.

The contribution of this article goes to: A framework design of cognitive tracking algorithm based on UKF, a robust method in cognitive structure developed to filter the uncertain noise faced by the traditional UKF, and more practical design with the supplemented robust mechanism for the cognitive radar system using for practical applications.

It is known that the noise covariance is related to the environment but the parameters are preset empirically [25], [33]. In the future work, a mathematical model of cognitive radar along with a new cost function is deserved to be built jointly by combining more variables, wherein the tuning parameters in the noise covariance update equation can be adaptive to the changing environment in real-time. Besides, the closed-form of the optimal solution of the biased cognitive estimation should be focused on, and using other new methods as the cognitive framework may have better prospects in dealing with the uncertain statistics.

APPENDIX A

The algorithm of UKF is well known and can be found elsewhere (e.g. [34]). In this appendix we restate the fundamental UKF equations to show the dependence of the UKF for CR on the cognitive waveform parameter $\boldsymbol{\theta}_k$, The equations are expressed as

1. Select an initial value of the filter

$$\hat{\mathbf{x}}_0 = E(\mathbf{x}_0) \tag{48}$$

$$\hat{\mathbf{P}}_0 = E\left[(\mathbf{x}_0 - \hat{\mathbf{x}}_0)(\mathbf{x}_0 - \hat{\mathbf{x}}_0)^T\right] \tag{49}$$

2. Calculate the sigma sample points

$$\chi_{(0)k-1} = \hat{\mathbf{x}}_{k-1} \tag{50}$$

$$\chi_{(j)k-1} = \hat{\mathbf{x}}_{k-1} + \sqrt{(n_x+\kappa)\hat{\mathbf{P}}_{k-1}} \quad j = 1, 2, \cdots, n_x \tag{51}$$

$$\chi_{(j)k-1} = \hat{\mathbf{x}}_{k-1} - \sqrt{(n_x+\kappa)\hat{\mathbf{P}}_{k-1}} \quad j = n+1, n+2, \cdots, 2n_x \tag{52}$$

where $\kappa = \alpha^2(n_x+\gamma) - n_x$, $10^{-4} \le \alpha \le 1$, $\gamma = 3 - n_x$.

3. Calculate the one-step prediction of the state and the covariance matrix

$$\chi_{(j)k|k-1} = \boldsymbol{f}\left(\chi_{(j)k-1}\right) \tag{53}$$

$$\bar{\mathbf{x}}_{k|k-1} = \sum_{j=0}^{2n_x} \boldsymbol{W}_j^{(m)} \chi_{(j)k|k-1} \tag{54}$$

$$\bar{\mathbf{P}}_{k|k-1} = \sum_{j=0}^{2n_x} \boldsymbol{W}_j^{(c)} \left[\chi_{(j)k|k-1} - \bar{\mathbf{x}}_{k|k-1}\right] \times \left[\chi_{(j)k|k-1} - \bar{\mathbf{x}}_{k|k-1}\right]^T + \mathbf{Q}_{k-1} \tag{55}$$

In cognitive radar, the state transition $\boldsymbol{f}\left(\chi_{(j)k-1}; \boldsymbol{\theta}\right)$ is used and $\bar{\mathbf{P}}_{k|k-1}(\boldsymbol{\theta})$ is obtained.

$$\boldsymbol{W}_0^{(m)} = \frac{\kappa}{n_x + \kappa} \tag{56}$$

$$\boldsymbol{W}_0^{(c)} = \frac{\kappa}{n_x+\kappa} + 1 - \alpha^2 + \beta \tag{57}$$

$$\boldsymbol{W}_j^{(m)} = \boldsymbol{W}_j^{(c)} = \frac{1}{2\left(n_x+\kappa\right)}, \quad j = 1, \ldots, 2n_x \tag{58}$$

where $\beta = 2$ for Gaussian distribution.

4. Define the update of measurement

$$\mathbf{z}_{(j)k|k-1} = \boldsymbol{h}\left(\chi_{(j)k|k-1}\right) \tag{59}$$

$$\bar{\mathbf{z}}_{k|k-1} = \sum_{j=0}^{2n_x} \boldsymbol{W}_j^{(m)} \mathbf{z}_{(j)k|k-1} \tag{60}$$

$$\begin{aligned}\bar{\mathbf{P}}_{k|k-1}^{zz}\left(\boldsymbol{\theta}\right) = &\sum_{j=0}^{2n_x} \boldsymbol{W}_j^{(c)} \left[\mathbf{z}_{(j)k|k-1} - \bar{\mathbf{z}}_{k|k-1}\right] \\ &\times \left[\mathbf{z}_{(j)k|k-1} - \bar{\mathbf{z}}_{k|k-1}\right]^T + \mathbf{R}_k\left(\boldsymbol{\theta}\right)\end{aligned} \tag{61}$$

$$\begin{aligned}\bar{\mathbf{P}}_{k|k-1}^{xz} = &\sum_{j=0}^{2n_x} \boldsymbol{W}_j^{(c)} \left[\chi_{(j)k|k-1} - \bar{\mathbf{x}}_{k|k-1}\right] \\ &\times \left[\mathbf{z}_{(j)k|k-1} - \bar{\mathbf{z}}_{k|k-1}\right]^T\end{aligned} \tag{62}$$

5. Calculate the gain and update the state and covariance

$$\hat{\mathbf{K}}_k = \bar{\mathbf{P}}_{k|k-1}^{xz}\left(\bar{\mathbf{P}}_{k|k-1}^{zz}\left(\boldsymbol{\theta}\right)\right)^{-1} \tag{63}$$

$$\mathbf{P}_k^{-}\left(\boldsymbol{\theta}\right) = \bar{\mathbf{P}}_{k|k-1} - \mathbf{K}_k \bar{\mathbf{P}}_{k|k-1}^{zz}\left(\boldsymbol{\theta}\right)\left(\mathbf{K}_k\right)^T \tag{64}$$

$$\hat{\mathbf{x}}_k^{-} = \bar{\mathbf{x}}_{k|k-1} + \mathbf{K}_k\left(\mathbf{z}_k - \bar{\mathbf{z}}_{k|k-1}\right) \tag{65}$$

In cognitive radar, here we find the minimum covariance to select the waveform parameter θ_k^* and confirm the state.

APPENDIX B

In this appendix, we restate the fault-detection mechanism and the one-step update method to show their work in the robust adaptive unscented Kalman filter and the cognitive cycle. The equations are expressed as

Input: $\boldsymbol{f}\left(\cdot\right), \boldsymbol{h}\left(\cdot\right), \hat{\mathbf{x}}_0, \mathbf{Q}_0, \mathbf{R}_1, \hat{\mathbf{P}}_0, \zeta_0, \delta_0, \boldsymbol{W}_0, \chi_{p,v}^2$

Initialization:

$$\chi_{(j)k-1} = \hat{\mathbf{x}}_{k-1} + \sqrt{\frac{n_x}{1-\boldsymbol{W}_j}\hat{\mathbf{P}}_{k-1}} \quad j = 1, 2, \cdots, n_x \tag{66}$$

$$\chi_{(j)k-1} = \hat{\mathbf{x}}_{k-1} - \sqrt{\frac{n_x}{1-\boldsymbol{W}_j}\hat{\mathbf{P}}_{k-1}} \quad j = n+1, n+2, \cdots, 2n_x \tag{67}$$

$$\boldsymbol{W}_j^{(m)} = \boldsymbol{W}_j^{(c)} = \boldsymbol{W}_j = \frac{1-\boldsymbol{W}_0}{2n_x} \tag{68}$$

Implement UKF as in Appendix A to obtain $\bar{\mathbf{P}}_{k|k-1}^{zz}\left(\boldsymbol{\theta}\right)$, $\mathbf{K}_k, \hat{\mathbf{P}}_{k|k}^{xx}$. Perform the fault-detection mechanism

$$\varphi_k = \boldsymbol{\mu}_k^T\left[\bar{\mathbf{P}}_{k|k-1}^{zz}\left(\boldsymbol{\theta}\right) - \mathbf{R}_k\left(\boldsymbol{\theta}\right)\right]^{-1}\boldsymbol{\mu}_k \tag{69}$$

If $\varphi_k > \chi_{p,v}^2$, then update the $\mathbf{Q}_{k-1}$ and $\mathbf{R}_k$

$$\boldsymbol{\mu}_k = \mathbf{z}_k - \boldsymbol{h}\left(\bar{\boldsymbol{x}}_{k|k-1}\right), \quad \boldsymbol{\varepsilon}_k = \mathbf{z}_k - \boldsymbol{h}\left(\hat{\mathbf{x}}_{k|k}\right) \tag{70}$$

$$\hat{\mathbf{S}}_{k|k}^{zz} = \sum_{j=0}^{2n_x} \boldsymbol{W}_j\left[\boldsymbol{h}\left(\chi_{(j)k|k}\right) - \bar{\mathbf{z}}_{k|k}\right] \times \left[\boldsymbol{h}\left(\chi_{(j)k|k}\right) - \bar{\mathbf{z}}_{k|k}\right]^T \tag{71}$$

$$\mathbf{Q}_{k-1} = \left(1-\zeta\right)\mathbf{Q}_{k-1} + \zeta\left(\mathbf{K}_k\boldsymbol{\mu}_k\boldsymbol{\mu}_k^T\mathbf{K}_k^T\right) \tag{72}$$

$$\mathbf{R}_k\left(\boldsymbol{\theta}\right) = \left(1-\delta\right)\mathbf{R}_k\left(\boldsymbol{\theta}\right) + \delta\left[\boldsymbol{\varepsilon}_k\left(\boldsymbol{\varepsilon}_k\right)^T + \hat{\mathbf{S}}_{k|k}^{zz}\right] \tag{73}$$

Correct the expected error covariance matrix

$$\mathbf{K}_k \triangleq \bar{\mathbf{P}}_{k|k-1}^{xz}\left(\bar{\mathbf{P}}_{k|k-1}^{zz}\left(\boldsymbol{\theta}\right)\right)^{-1} \tag{74}$$

$$\hat{\mathbf{P}}_{k|k}^{xx}\left(\boldsymbol{\theta}\right) = \hat{\mathbf{P}}_{k|k}^{xx} + \hat{\mathbf{K}}_k\bar{\mathbf{P}}_{k|k}^{zz}\left(\boldsymbol{\theta}\right)\left(\hat{\mathbf{K}}_k\right)^T \tag{75}$$

$$\mathbf{Q}_k = \mathbf{Q}_{k-1}, \mathbf{R}_{k+1}\left(\boldsymbol{\theta}\right) = \mathbf{R}_k\left(\boldsymbol{\theta}\right)$$

Save $\hat{\mathbf{P}}_{k|k}^{xx}$

ACKNOWLEDGMENT

The authors would like to thank editors and reviewers for their helpful advice and comments. They would also like to thank Zhizheng Xu with the Dalian University of Technology and Moin Akhtar and Chenxi Liu with Northwestern Polytechnical University for their helpful advice on revision.

REFERENCES

[1] S. Haykin, "Cognitive radar: A way of the future," *IEEE Signal Process. Mag.*, vol. 23, no. 1, pp. 30–40, Jan. 2006.

[2] J. R. Guerci, "Introduction," in *Cognitive Radar: The Knowledge-Aided Fully Adaptive Approach*, vol. 2. Norwood, MA, USA: Artech House, 2010, pp. 14–16.

[3] K. L. Bell, C. J. Baker, G. E. Smith, J. T. Johnson, and M. Rangaswamy, "Cognitive radar framework for target detection and tracking," *IEEE J. Sel. Top. Signal Process.*, vol. 9, no. 8, pp. 1427–1439, Dec. 2015.

[4] G. E. Smith, "Experiments with cognitive radar," *IEEE Aerosp. Electron. Syst. Mag.*, vol. 31, no. 12, pp. 34–46, Dec. 2016.

[5] G. Rossetti and S. Lambotharan, "Robust waveform design for multistatic cognitive radars," *IEEE Access*, vol. 6, pp. 7464–7475, 2018.

[6] T. Hao, C. Cui, and Y. Gong, "Efficient waveform design method for target estimation under the detection and Peak-to-Average power ratio constraints in cognitive radar," *IEEE Access*, vol. 7, pp. 21300–21309, 2019.

[7] A. M. Elbir, K. V. Mishra, and Y. C. Eldar, "Cognitive radar antenna selection via deep learning," *IET Radar, Sonar Navigat.*, vol. 13, no. 6, pp. 871–880, Jun. 2019.

[8] Y. Xue, "Cognitive Radar: Theory and Simulations," Ph.D. dissertation, Dept. Elect. Comput. Eng., McMaster Univ., Hamilton, ON, Canada, 2010.

[9] K. L. Bell, J. T. Johnson, G. E. Smith, C. J. Baker, and M. Rangaswamy, "Cognitive radar for target tracking using a software defined radar system," in *Proc. IEEE Radar Conf. (RadarCon)*, Arlington, VA, USA, May 2015, pp. 1394–1399.

[10] D. Avila, E. Alvarez, and A. Abusleme, "Noise analysis in pulse-processing discrete-time filters," *IEEE Trans. Nucl. Sci.*, vol. 60, no. 6, pp. 4634–4640, Dec. 2013.

[11] L. Zhong, Y. Li, W. Cheng, and Y. Zheng, "Cost-reference particle filter for cognitive radar tracking systems with unknown statistics," *Sensors*, vol. 20, no. 13, p. 3669, Jun. 2020.

[12] H. Fourati and K. Iniewski, "Data fusion in intelligent traffic and transportation engineering: Recent advances and challenges," in *Multisensor Data Fusion: From Algorithms and Architectural Design to Applications*, vol. 6. Boca Raton, FL, USA: CRC Press, 2015, pp. 574–577.

[13] C. Hajiyev and H. E. Soken, "A novel adaptive unscented Kalman filter for pico satellite attitude estimation," in *Proc. 5th International Conference on Physics and Control*, León, Spain, Sep. 2011, pp. 1–9.

[14] S. Peng, X. Zhu, Y. Xing, H. Shi, X. Cai, and M. Pecht, "An adaptive state of charge estimation approach for lithium-ion series connected battery system," *J. Power Sources*, vol. 392, pp. 48–59, 2018.

[15] S. Peng, C. Chen, H. Shi, and Z. Yao, "State of charge estimation of battery energy storage systems based on adaptive unscented Kalman filter with a noise statistics estimator," *IEEE Access*, vol. 5, pp. 13202–13212, 2017.
[16] T. Ardeshiri, E. Ozkan, U. Orguner, and F. Gustafsson, "Approximate Bayesian smoothing with unknown process and measurement noise covariances," *IEEE Signal Process. Lett.*, vol. 22, no. 12, pp. 2450–2454, Dec. 2015.
[17] Q. Xu, X. Li, and C.-Y. Chan, "A cost-effective vehicle localization solution using an interacting multiple model unscented Kalman filters (IMM-UKF) algorithm and grey neural network," *Sensors*, vol. 17, no. 6, p. 1431, Jun. 2017.
[18] A. Assa and K. N. Plataniotis, "Adaptive Kalman filtering by covariance sampling," *IEEE Signal Process. Lett.*, vol. 24, no. 9, pp. 1288–1292, Sep. 2017.
[19] L. Zanni, J.-Y. Le Boudec, R. Cherkaoui, and M. Paolone, "A prediction-error covariance estimator for adaptive Kalman filtering in step-varying processes: Application to power-system state estimation," *IEEE Trans. Control Syst. Technol.*, vol. 25, no. 5, pp. 1683–1697, Sep. 2017.
[20] F. A. Ghaleb, A. Zainal, M. A. Rassam, and A. Abraham, "Improved vehicle positioning algorithm using enhanced innovation-based adaptive Kalman filter," *Pervas. Mobile Comput.*, vol. 40, pp. 139–155, Sep. 2017.
[21] N. Davari and A. Gholami, "An asynchronous adaptive direct Kalman filter algorithm to improve underwater navigation system performance," *IEEE Sensors J.*, vol. 17, no. 4, pp. 1061–1068, Feb. 2017.
[22] S. Gao, G. Hu, and Y. Zhong, "Windowing and random weighting-based adaptive unscented Kalman filter," *Int. J. Adapt. Control Signal Process.*, vol. 29, no. 2, pp. 201–223, Feb. 2015.
[23] C. Hajiyev and H. E. Soken, "Robust adaptive unscented Kalman filter for attitude estimation of pico satellites," *Int. J. Adapt. Control Signal Process.*, vol. 28, no. 2, pp. 107–120, Feb. 2014.
[24] W. Li, S. Sun, Y. Jia, and J. Du, "Robust unscented Kalman filter with adaptation of process and measurement noise covariances," *Digit. Signal Process.*, vol. 48, pp. 93–103, Jan. 2016.
[25] B. Zheng, P. Fu, B. Li, and X. Yuan, "A robust adaptive unscented Kalman filter for nonlinear estimation with uncertain noise covariance," *Sensors*, vol. 18, no. 3, p. 808, Mar. 2018.
[26] D. J. Kershaw and R. J. Evans, "Optimal waveform selection for tracking systems," *IEEE Trans. Inf. Theory*, vol. 40, no. 5, pp. 1536–1550, 1994.
[27] H. L. Van Trees, "Estimation of the Parameters of a Random Process," in *Detection, Estimation, and Modulation Theory, Part III: Radar-sonar signal processing and Gaussian signals in Noise*, vol. 3. New York, NY, USA: Wiley, 2001, pp. 177–184.
[28] D. J. Kershaw and R. J. Evans, "Waveform selective probabilistic data association," *IEEE Trans. Aerosp. Electron. Syst.*, vol. 33, no. 4, pp. 1180–1188, Oct. 1997.
[29] J. Wang, Y. Qin, H. Wang, and X. Li, "Dynamic waveform selection for manoeuvering target tracking in clutter," *IET Radar, Sonar Navigat.*, vol. 7, no. 7, pp. 815–825, Aug. 2013.
[30] Y. Bar-Shalom, X. R. Li, and T. Kirubarajan, "Adaptive estimation and maneuvering targets," in *Estimation With Applications to Tracking and Navigation*, vol. 7. New York, NY, USA: Wiley, 2001, pp. 466–476.
[31] S. M. Kay, "Maximum likelihood estimation," in *Fundamentals Statistical Signal Processing: Estimation Theory*, vol. 1. Upper Saddle River, NJ, USA: Prentice-Hall, 2007, pp. 164–173.
[32] B. R. Mahafza, "Radar systems—An overview," in *Radar Signal Analysis and Processing using MATLAB*, vol. 10. Boca Raton, FL, USA: Chapman Hall, 2016, pp. 53–58.
[33] X. Luo and H. Wang, "Robust adaptive Kalman filtering-a method based on quasi-accurate detection and plant noise variance-covariance matrix tuning," *J. Navigat.*, vol. 70, p. 137, 2017.
[34] A. J. Haug, "The sigma point class: The unscented Kalman filter," in *Bayesian Estimation Tracking: A Practical Guide*, vol. 2. Hoboken, NJ, USA: Wiley, 2012, pp. 130–136.

LEI ZHONG (Member, IEEE) received the M.S. degree from the School of Information Engineering, Dalian University, Liaoning, China, in 2013. He is currently pursuing the Ph.D. degree in information and communication engineering with Northwestern Polytechnical University, Xi'an, China.

His research interests include cognitive radar, communication and signal processing, and multi-sensor information fusion.

YONG LI received the B.S. degree in avionics engineering and the M.S. and Ph.D. degrees in circuits and systems from Northwestern Polytechnical University, Xi'an, China, in 1983, 1988, and 2005, respectively.

He joined the School of Electronic Information, Northwestern Polytechnical University, in 1993, where he was promoted to a Professor, in 2002. His research interests include digital signal processing and radar signal processing.

WEI CHENG received the B.S. degree in electronic and information engineering and the M.S. and Ph.D. degrees in communication and information system from Northwestern Polytechnical University, Xi'an, China, in 2003, 2006, and 2011, respectively.

From April 2011 to April 2013, he worked with the Postdoctoral Research Station, School of Electronic Information, Northwestern Polytechnical University, where he has been a Lecturer, since 2013, and was promoted to an Associate Professor, in 2015. His research interests include wireless sensor networks, *ad hoc* networks, and radar signal processing.

WEI ZHOU received the B.S. degrees in electronic and information engineering and communication and information system from Northwestern Polytechnical University, Xi'an, China, in 2017, where he is currently pursuing the M.S. degree in communication and information system.

His research interests include software-defined radio and radar signal processing.